Mediterranean Marine Science

Vol 21, No 3 (2020)

Vol 21, n3

Approaches to evaluate spatial and temporal variability of deep marine sediment characteristics under the impact of dense water formation events

XAVIER DURRIEU de MADRON, MARION STABHOLZ, LARS-ERIC HEIMBÜRGER-BOAVIDA, DOMINIQUE AUBERT, PHILIPPE KERHERVÉ, WOLFGANG LUDWIG

doi: 10.12681/mms.22581

Research Article

Mediterranean Marine Science
Indexed in WoS (Web of Science, ISI Thomson) and SCOPUS
The journal is available on line at http://www.medit-mar-sc.net
DOI: http://dx.doi.org/10.12681/mms.22581

Approaches to evaluate spatial and temporal variability of deep marine sediment characteristics under the impact of dense water formation events

Xavier DURRIEU de MADRON[1], Marion STABHOLZ[1], Lars-Eric HEIMBÜRGER-BOAVIDA[2], Dominique AUBERT[1], Philippe KERHERVE[1], Bruno CHARRIERE[1] and Wolfgang LUDWIG[1]

[1] CEFREM, CNRS-Université de Perpignan Via Domitia, 52 avenue Paul Alduy, 66860 Perpignan Cedex, France
[2] Aix Marseille Université, CNRS, Université de Toulon, IRD, Mediterranean Institute of Oceanography (MIO) UM 110, 13288, Marseille, France

Corresponding author: demadron@univ-perp.fr

Handling Editor: Elina TRAGOU

Received: 17 March 2020; Accepted: 29 July 2020; Published on line: 9 September 2020

Abstract

Dense shelf water cascading and open-ocean convection frequently occur in the Gulf of Lions, Northwestern Mediterranean Sea. These intense dense water formation events are capable of supplying large amounts of particulate matter as well as remobilizing and dispersing local sediments and are therefore thought to leave an imprint on superficial deposits. Here, we compare the spatial variability of the superficial sediment composition (grain size, organic parameters, and metals) at different scales (from decimetric to kilometric) on the continental slope and rise with the temporal variability linked to the occurrence of intense dense water formation events. The spatial and temporal variability of the geochemical composition of deep sediments was assessed using multivariate and geostatistical analyses. The results indicate that in the outer reaches of Cap de Creus Canyon, where both processes interact, no clear relation was found between the temporal variability of the superficial sediment and the deep-water formation events, and that the small-scale spatial variability of the sediment masks the temporal variability. Measurements across the southern slope indicate the presence of a somewhat distinct geochemical signature that likely results from the influence of recurrent intense, dense water formation events as well as unabating bottom trawling activity.

Keywords: Submarine canyon; organic matter; trace metals; Mediterranean; winter convection; bottom trawling.

Introduction

Continental margins are areas where shelf/slope exchanges of sediment and associated organic/inorganic elements play a significant role in the global biogeochemical cycles of nutrients and contaminants. Deep-sea sediments are considered as final sinks for both particulate organic matter, which is degraded neither in the water column nor at the water-sediment interface (Lochte *et al.*, 2003), and for many associated contaminants (Olsen *et al.*, 1982). Deep sediments have generally been considered to be relatively stable/inert, and measurement strategies typically consist of low resolution sampling. However, various hydrodynamic processes (e.g., internal waves, along-slope current meanders and eddies, current-canyon interactions, storm-induced downwelling, dense shelf water cascading) which are involved in the export of water and particulate matter from the coastal zone or the offshore surface layer to the slope and basin, are also active in deep environments, and thus control the distribution of chemical elements that settle on the seabed. It is readily conceivable that the geochemical composition of deep sediments is susceptible to evolve according to the recurrence and intensity of inputs, but also in relation to the removal of material induced by strong currents affecting the deep slope and basin, especially during abyssal storm events. If inputs predominate over removal, the development of a distinct signature of the superficial sediment is expected to testify to the effect of an event or a series of events. Such changes are well known in the coastal environment, especially under the influence of floods and storms (Durrieu de Madron *et al.*, 2008), but have not been sufficiently addressed in deep-sea environments.

The Gulf of Lions (GoL), in the Northwestern Mediterranean Sea, is a particularly dynamic margin where strong physical forcing prevails and where episodic events such as storms and dense water formation (DWF) repeatedly occur. DWF, which is due mainly to the effect of active and persistent northerly dry winds (Mistral and Tramontane) in winter, occurs both on the shelf, where off-shelf export is known as dense water shelf cascading (DSWC), and in the open ocean, resulting in open-ocean

convection (OOC) (Béthoux *et al.*, 2002 ; Durrieu de Madron *et al.*, 2013) (Fig. 1).

DSWC shows a strong interannual variability and is an essential mechanism for sediment-transport and resuspension on the shelf-slope. River inputs of particulate organic matter and metals, initially sequestered in shelf sediments, are eventually remobilized and exported toward the slope and the basin during these events (Durrieu de Madron *et al.*, 2008 and references therein). While plumes of dense and turbid coastal water generally reach depths of a few hundred meters on the slope, occasional formation of very dense coastal water provokes the rapid propagation of the plumes down to the base of the slope and eventually into the basin (Durrieu de Madron *et al.*, 2005, 2013 ; Canals *et al.*, 2006 ; Palanques *et al.*, 2012; Palanques & Puig, 2018). The open-slope south of Cap de Creus Canyon, which is the main export pathway for dense water formed on the shelf, thus appears as a region where recurrent deposition of exported matter could potentially occur. Occasional deep DSWC events, observed in the southwesternmost canyons of the GoL, displace erodible sediment from the upper- and mid-canyons to their lower reaches (Canals *et al.*, 2006; Palanques *et al.*, 2012; Sanchez-Vidal *et al.*, 2009; Pasqual *et al.*, 2010; Puig *et al.*, 2013).

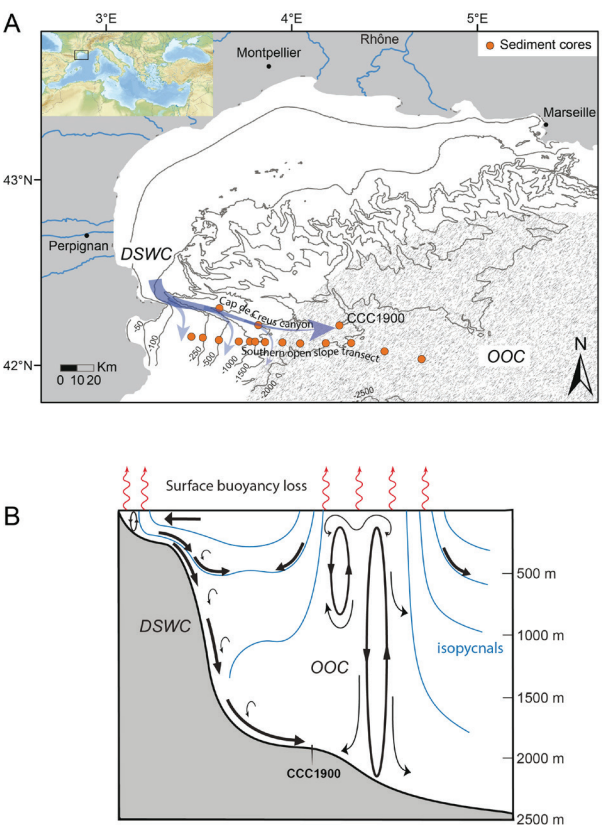

Fig. 1: (A) Map of the study area topography and sampling locations (circles) along the two bathymetric transects of Cap de Creus Canyon and its Southern Open Slope. The blue arrow represents the trajectory of dense water flow formed on the continental shelf, cascading down Cap de Creus Canyon or overflowing onto the open slope. The hatched area delimits the area affected by open ocean convection. (B) Schematic cross-section across the shelf, slope and basin illustrating the juxtaposition of coastal dense water formation and cascading down the slope, and offshore convective mixing.

OOC covers a large part of the NW Mediterranean deep basin offshore of the GoL and affects regions of the continental slope from a depth of 1500 m and deeper (Testor *et al.*, 2018). Bottom-reaching OOC (down to 2500 m depth) affects particulate matter transport and sediment dynamics. During the phases of vigorous mixing and spreading of newly formed deep water, the deep basin is impacted by strong bottom currents (up to 50 cm/s) that resuspend and disperse seabed sediment (Stabholz *et al.*, 2013 ; Durrieu de Madron *et al.*, 2017; Palanques & Puig, 2018).

On the deep slope and rise, DSWC and OOC events are believed to modify the characteristics of deep-sea sediments by supplying large amounts of particulate matter as well as remobilizing and dispersing the local sediment. Any alteration of deep sediment composition (e.g., particulate organic carbon (POC), total nitrogen (TN)) has consequences for deep marine ecosystems (Pusceddu *et al.*, 2010, 2013; Nardelli *et al.*, 2018). Furthermore, the accumulation of organic contaminants found at the base of the Lacaze-Duthiers and Cap de Creus Canyons is in agreement with predominant transport by OOC convection and DSWC episodes (Salvadó *et al.*, 2012, 2013). Regarding trace elements, it is also now well recognized that marine sediments act as sinks for metallic contaminants (Valette-Silver, 1993) and can constitute archives for monitoring past contamination (Lopes-Rocha *et al.*, 2017). In our study area, metals (both natural and anthropogenic) can be transferred by rivers, temporarily stored on the shelf (Roussiez *et al.*, 2006) and then be flushed into canyons during DSCW or storms (Dumas *et al.*, 2014; Roussiez *et al.*, 2012). Cossa *et al.* (2014) used particle trap samples collected between October 2004 and May 2005 and sediment cores collected in October 2005 in Cap de Creus Canyon and on its adjacent open-slope, to show that the major DSWC event of winter 2005 had transported down the slope particles which were coarser and slightly metal-depleted when compared to the clays and organic-rich particles deposited before and after the event. On the contrary, in offshore and deep open sea sediments, atmospheric deposition is thought to be another critical source of metal accumulation (Miralles *et al.*, 2006; Martín *et al.*, 2009; Angelidis *et al.*, 2011), and dense water convection and primary production have been shown to control marine vertical export flux (Heimbürger *et al.*, 2014).

The primary objective of our study is to characterize the possible imprint left on deep sediment composition by energetic hydrodynamical and particulate matter transport events, such as DSWC and OOC. This study presents two complementary approaches. The first is based on pluriannual monitoring at a deep station in an attempt to correlate the geochemical changes of superficial sediment with the DSWC and OOC events observed during the measurement period. The second is rooted in the study of spatial variability along a section across the continental slope, regularly (annually) affected by variable DSWCs, to detect whether the parts of the

most frequently impacted slope present a different geochemical signature. Incidentally, we estimated the spatial heterogeneity at small scales (from decimeters to kilometers) and used it to interpret the representativeness of each approach.

Materials and Methods

Sediment sampling

Sediment samples were collected with an OKTOPUS multiple-corer (Barnett *et al.*, 1984), equipped with eight polycarbonate tubes (9 cm diameter and 70 cm length). This device is typically used to sample the sediment-water interface. All cores were carefully sliced onboard in 0.5 cm layers from the surface to 5 cm depth using acid-cleaned plastic spatulas, stored in polyethylene plastic bags and kept at 4° C until the return to the laboratory. Samples were frozen, freeze-dried, then crushed and homogenized using an agate mortar before analysis. Organic carbon, total nitrogen, total carbon, metals, and grain size were analysed for all surface sediment samples (0 - 0.5 cm).

Regarding monitoring of temporal variability, surface sediments were sampled at the CC1900 site which is located at 1900 m depth at the convergence of the Lacaze-Duthiers and Cap de Creus Canyons, where both DSWC and OOC can be observed (Palanques *et al.*, 2012). Annual sampling began in 2005 after an intense DSWC event, and ended in 2010. The sampling periods are October 2005, August 2006, April 2008, October 2008, April 2009, October 2009, and November 2010. During these five years, deep DSWC events occurred in winters 2005 and 2006 (Canals *et al.*, 2006; Palanques *et al.*, 2012). OOC events were observed in winters 2005, 2006, 2009, and 2010 (Stabholz *et al.*, 2013; Houpert *et al.*, 2016; Somot *et al.*, 2016).

Core position was determined by the position of the vessel when the multi-tube corer touched bottom. Distances of core positions from the median location associated with the temporal sampling at site CCC1900 are presented in Figure 2A. The distance between the successive cores ranged from a few meters to 700 m. Given that the ability to detect changes in environmental parameters depends on the variance associated with measurements and sampling, we conducted a complementary study at this location to address the small-scale spatial variability of the sediment. A comparative hierarchical sampling of 27 cores was undertaken in April 2009. Nine "deployments" (D1 to D9) were performed at three sites (S1 at 1950 m-depth, S2 at 1955 m-depth, S3 at 1962 m-depth) in the vicinity of site CCC1900 (Figure 2B). Three cores were collected from each multicorer deployment (D), resulting in 27 cores with individual distances between cores ranging from a few tens of centimeters to several hundred meters.

Seventeen stations were sampled in October 2009 in order to better understand the impact of recurrent dense water flows on the surface sediment in Cap de Creus

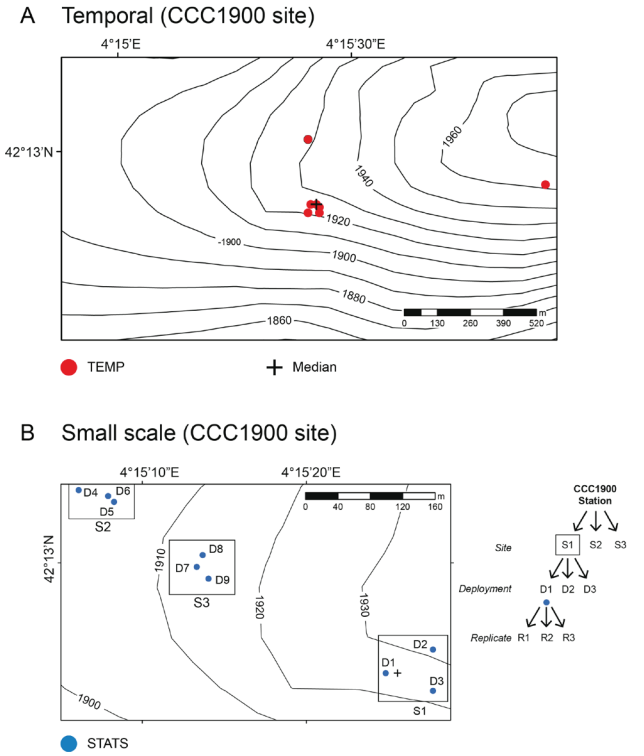

Fig. 2: Sampling area at coring site CCC1900 situated at the convergence of Lacaze-Duthiers Canyon and Cap de Creus Canyon (see Fig. 1). (A) Location of the successive temporal sampling performed between October 2005 and November 2010 ("Temp" red dots) and its median position (black cross). (B) Close up of the location of the small-scale hierarchical sampling design (blue dots represent each deployment location, and open squares delimit each site) performed in April 2009. Isobaths are drawn at 10m intervals.

Canyon and on its southern open slope. The stations are located along two bathymetric transects, one inside Cap de Creus Canyon from 1000 to 1900 m water depth and the second along the Southern Open Slope from 150 to 2350 m depth (Fig. 1).

Geochemical analyses

Grain size distribution

Grain size analysis was performed using a Malvern Mastersizer 2000 laser diffraction particle size analyzer. Aliquots of fresh bulk top sediment were made with 500 mL of deionized water to obtain suspensions in a suitable dispersion to carry out the measurements. A short ultrasonic treatment was applied to break up loose aggregates. For each sample, two dispersions were prepared, and the procedure was repeated three times until a stable dispersion was achieved. Measurable sizes ranged from 50 nm to 1000 µm, and the results were then classified based on textural features according to the Udden-Wentworth scale in three main categories: clay <4 µm, 4 µm ≤ silt <63 µm, and 63 µm <sand <1 mm.

Particulate organic carbon (POC) and total nitrogen (TN) analysis

The subsamples (20 to 50 mg) used for elemental (POC and TN) and isotopic ($\delta^{13}C$ and $\delta^{15}N$) analyses were freeze-dried and ground to a fine powder. Samples for POC and $\delta^{13}C$ analyses were decarbonated using repeated additions of 25% HCl until no effervescence was observed. POC and TN were measured by high-temperature combustion on decarbonated and raw filters, respectively, using a LECO CN 2000. At least two replicates were analysed for each sample. Uncertainties were lower than ±2% for POC, and less than ±0.2% for TN samples as determined from replicates of IAEA certified soil materials (soil-7 and Soil-4). The POC and TN concentrations are expressed in percent of the dry sediment mass.

Stable Carbon and Nitrogen isotopes

Free-carbonate and raw samples were placed in tin capsules to determine the stable isotope composition of POC ($\delta^{13}C_{POC}$) and TN ($\delta^{15}N$), respectively, using a Eurovector Elemental Analyzer coupled to a GVI-Isoprime Isotope Ratio Mass Spectrometer (EA-IRMS). Uncertainties were lower than 0.2‰ as determined from routine replicate measurements of the IAEA reference samples CH-3 (-24.5‰) for $\delta^{13}C_{POC}$ and N-1 (-0.4‰) for $\delta^{15}N$. Isotope data are expressed in per mil (‰) relative to Vienna Pee Dee Belemnite for $\delta^{13}C_{POC}$ and atmospheric N_2 for $\delta^{15}N$.

Trace metals: Al, Cu, Pb, and Hg

Aluminium is often considered as a proxy for clay minerals (or fine silts) that are efficient carriers of trace metals (Loring, 1991) together with their coatings involving organic matter, for instance. We verified that the pelitic fraction (grain size <63 µm) and aluminium concentrations of all surface sediment samples were significantly correlated. Aluminium normalization was then used to identify fluctuations of metals in detrital alumino-silicate source materials (Van der Weijden, 2002), mostly at site CCC1900, where the linear relationship (%(Clays+Silts) = 1.053 × %Al + 28.36) is obtained with a significant correlation coefficient of 0.82 (n = 40). Regarding contaminants, we chose to monitor lead, which has been widely released into the marine environment for almost two centuries as a result of anthropogenic activities (Cossa *et al.*, 2014). Copper represents a more local concern due to its intensive use as an agricultural fungicide in the South of France (Panogos *et al.*, 2018), a practice that can lead to the significant export of this element to the Mediterranean Sea through runoff or atmospheric deposition.

Freeze-dried aliquots of bulk sediment samples were mineralized in Teflon beakers with a mixture of high quality (trace metal grade) nitric and hydrofluoric acids (HNO_3-HF) and oxygen peroxide (H_2O_2). Major and trace element concentrations were measured by Inductively Coupled Plasma Mass Spectrometry (ICP-MS, Agilent 7000x). Marine sediment reference materials (GSMS-2 and GSMS-3 from NRCGA-CAGS, China) were mineralized and analysed under the same conditions as the samples and provided suitable recoveries (errors <5% for all elements). Analytical blanks were always negligible.

Particulate mercury was measured by atomic absorption spectrophotometry (AAS) using a LECO AMA-254. The instrument was calibrated with marine sediment standard reference material MESS-4 provided by the National Research Council Canada. During analyses, MESS-4 was measured every ten samples to verify calibration, and procedural blanks were measured every five samples. MESS-4 concentrations were always within the range of certified values of 90 ± 4 ng/g. Duplicate Hg measurements were made on selected samples to assess the reproducibility of the analyses (maximum of 10% variability for all duplicated samples).

Statistical analyses

Permanova

Both univariate and multivariate nonparametric permutational ANOVAs (PERMANOVA) based on Bray-Curtis dissimilarity (Anderson, 2001; Anderson & Braak, 2003; Anderson & Robinson, 2003) are robust alternatives to the parametric multivariate analysis of variance. They were used here to test for differences in the geochemical composition of sediment between sites and between deployments relating to the same site. Multivariate data were analysed based on any distance measure, according to any linear ANOVA model, using permutations. Random factor 1 (the site) has three levels; random factor 2 is nested within factor 1 and also has three levels, the sample size is 3 (n = 3 core replicates within a deployment). Calculation of the F-ratio and p-value required unrestricted permutations of raw data (univariate), or 4999 permutations of the residuals under a reduced model (multivariate). The set of data used in the multivariate PERMANOVA test was POC content (%), $\delta^{13}C_{POC}$ (‰), TN content (%), $\delta^{15}N$ (‰), Al (%), Cu (µg/g), Hg (ng/g), and Pb (µg/g) concentrations. POC content, $\delta^{13}C$ (‰), TN content (%), $\delta^{15}N$ (‰), Al (%), Cu/Al, Hg/Al, and Pb/Al ratios were used for univariate PERMANOVA analysis. The test examined possible occurrences of significant ($p < 0.05$) variability (differences) of a given variable among coring sites (S1, S2, S3) and deployments (D1 to D9) within a coring site.

Semi-variogram

Common descriptive statistics do not incorporate the spatial locations of data. For this reason, we used a geostatistical tool, the semi-variogram, to better analyse the spatial variability of measurements. The semi-variogram,

is half the mean of the squares of the differences between pairs of values, $z(x_i)$ and $z(x_i+h)$, separated by the distance h.

We used the variogram function of Matlab® software for our data.

Box Plot

For each variable, the main features of data variability observed within our sampling scheme were graphically represented by box plots of small (STATS) and large (TRANSECT) spatial scales, and temporal scale (TEMP). Each box encloses 50% of the data around the median value. The top (upper quartile) and bottom (lower quartile) of the box mark the limits of ± 25% of the data population around the median; the bottom and top lines outside the box mark the minimum and maximum values, respectively, of the data set that fall within an acceptable range (95% of data). Any outliers (values outside this range), are displayed as individual points.

Kruskal-Wallis test

This nonparametric test (one-way analysis of variance on ranks) was used to perform multiple comparisons of the STATS, TEMP and TRANSECT groups (Georgin & Mouet, 2000). Their ranks in the data series replace absolute values. The calculated p-value determines if there is a statistically significant difference (threshold $\alpha = 0.05$) between the median of the groups. If $p < 0.05$, the conclusion is that there is a difference between the groups. When significant differences between groups are observed, post-hoc pairwise tests (Siegel & Castellan, 2002) can be performed to determine which groups are different.

Results

Surface and down core granulometry

The surface sediment across the slope and at site CCC1900 is mostly composed by clays and silts.

Grain size distribution was the only parameter measured downcore on the 27 cores at CCC1900 (Table 1). Over a thickness of 10 cm, mean clay content varied from 20.6 to 33.0%, mean silt content from 49.2 to 54.1%, and mean sand content from 14.1 to 25.3%. The stronger variability was observed in the upper 1.5 cm; clays varied between 11.0 and 35.3%, silts between 17.2 and 66.7%, and sands between 12.6 and 71.8%. Below 1.5 cm depth, the clay, silt and sand contents stabilized at approximately

Table 1. Downcore variability of Clay, Silt and Sand contents for the 27 replicated cores at the CCC1900 site. See Figure 2B for the location of the cores.

Core depth (cm)		Clay (%)	Silt (%)	Sand (%)	D50 (µm)
0 - 0.5	Mean ± std dev	20.6 ± 4.8	54.1 ± 6.1	25.3 ± 9.1	14.8 ± 9.3
	Range	(11.5 - 29.4)	(33.9 - 66.7)	(14.5 - 52.8)	(8.0 - 52.5)
0.5 - 1	Mean ± std dev	27.4 ± 5.1	51.8 ± 3.3	20.8 ± 6.2	9.6 ± 3.1
	Range	(12.9 - 34.2)	(43.0 - 57.5)	(12.9 - 34.8)	(6.7 - 19.2)
1 - 1.5	Mean ± std dev	29.6 ± 5.1	49.2 ± 7.3	21.2 ± 11.7	8.2 ± 1.3
	Range	(11.0 - 35.3)	(17.2 - 54.3)	(12.6 - 71.8)	(6.4 - 11.5)
1.5 - 2	Mean ± std dev	32.1 ± 2.8	50.2 ± 1.9	17.7 ± 3.8	7.8 ± 1.1
	Range	(25.3 - 37.2)	(45.0 - 53.0)	(10.9 - 24.8)	(6.2 - 11.3)
2 - 2.5	Mean ± std dev	32.2 ± 2.4	50.5 ± 2.5	17.3 ± 3.8	7.9 ± 1.1
	Range	(25.5 - 36.6)	(46.6 - 56.5)	(11.0 - 25.8)	(6.3 - 11.0)
2.5 - 3	Mean ± std dev	32.1 ± 2.0	49.9 ± 3.3	18.0 ± 4.6	8.0 ± 0.9
	Range	(27.7 - 35.1)	(42.4 - 57.2)	(10.4 - 28.0)	(6.9 - 10.3)
3 - 3.5	Mean ± std dev	32.2 ± 1.8	50.2 ± 3.4	17.6 ± 3.8	8.0 ± 0.8
	Range	(29.1 - 36.4)	(44.4 - 59.7)	(9.6 - 24.7)	(6.5 - 9.7)
3.5 - 4	Mean ± std dev	32.6 ± 2.2	50.9 ± 4.0	16.4 ± 4.2	8.0 ± 1.0
	Range	(28.0 - 36.2)	(44.4 - 60.9)	(8.9 - 24.2)	(6.4 - 10.9)
4 - 4.5	Mean ± std dev	32.1 ± 2.3	51.3 ± 4.7	16.6 ± 5.4	8.4 ± 1.5
	Range	(26.8 - 35.9)	(40.6 - 62.2)	(9.6 - 32.6)	(6.6 - 14.1)
4.5 - 5	Mean ± std dev	32.3 ± 2.2	51.7 ± 4.0	16.0 ± 4.2	8.3 ± 1.3
	Range	(25.5 - 35.6)	(44.9 - 60.5)	(8.6 -24.0)	(6.6 - 13.2)
5 - 6	Mean ± std dev	32.2 ± 2.8	52.4 ± 3.5	15.4 ± 4.1	8.4 ± 1.6
	Range	(25.8 - 35.8)	(46.5 - 60.1)	(8.0 -23.3)	(6.4 - 13.8)
6 - 7	Mean ± std dev	32.0 ± 2.7	52.9 ± 3.5	15.1 ± 4.1	8.8 ± 2.1
	Range	(26.1 - 36.1)	(43.0 - 58.9)	(6.5 - 24.0)	6.4 - 15.1)
7 - 8	Mean ± std dev	33.0 ± 2.3	52.9 ± 3.2	14.1 ± 3.7	8.0 ± 1.1
	Range	(27.5 - 37.2)	(46.9 - 60.6)	4.7 - 22.1)	(6.1 - 11.2)
8 - 9	Mean ± std dev	32.5 ± 3.9	52.1 ± 3.4	15.4 ± 6.4	9.2 ± 4.6
	Range	(21.7 - 37.2)	(40.5 - 56.3)	(9.1 - 32.9)	(6.2 - 24.1)
9 - 10	Mean ± std dev	31.9 ± 4.4	52.2 ± 3.9	15.9 ± 7.4	10.3 ± 8.4
	Range	(19.6 - 37.3)	(42.0 - 57.9)	(8.6 - 38.4)	(6.3 - 43.6)

32%, 52% and 15%, respectively. These results emphasize that recent perturbations of the sediment are confined to the uppermost layer of the cores before background values are reached. This critical information led us to study only the upper 0.5 cm (the surficial sediment), which is the layer most likely to have been modified by extreme events such as DSWC and OOC, as well as by bioturbation.

As will be shown later, the grain size of the surficial sediment is highly variable, both spatially and temporally. The bias effect induced by changes in grain size has been reduced by calculating the ratio of metal content to aluminium content because the pelitic fraction (% clays + silts) is well correlated with aluminium.

Interannual variability of surface sediment at site CCC1900 (TEMP)

Superficial sediment (0–0.5 cm) was composed of silty loam (clays ~ 27%, silts ~ 57%, sands ~ 16%). Figure 3 and Table 2 present the temporal variability of each parameter between October 2005 and November 2010. The temporal variability of the different parameters at station CCC1900 revealed no common trends nor any clear impact of DWF events. The anticipated disrupting effect of the intense DSWC and OOC events of winters 2005 and 2006 in terms of particulate organic matter inputs, is not visible. Despite the increase of POC and TN content between 2005 and 2006, the subsequent variability -in the absence of deep DSWC- is of similar magnitude. Moreover, the occurrence of bottom-reaching OOC during winters 2009 and 2010 once again reveals no coherent or substantial changes in geochemical parameters.

The temporal variability of the different elements clearly contrasts. POC contents ranged between 0.37 (November 2010) and 0.54% (April 2008). TN contents ranged between 0.028 (November 2010) and 0.069% (October 2009). $\delta^{13}C_{POC}$ ranged between -22.11 (April 2008) and -22.57‰ (April 2009) and $\delta^{15}N$ ranged between 3.67 (November 2010) and 4.60‰ (October 2005). November 2010 was a period with organic-depleted surface sediments. Al ranged between 3.10% (April 2008) and 5.78% (November 2010), Cu/Al ranged between 4.18

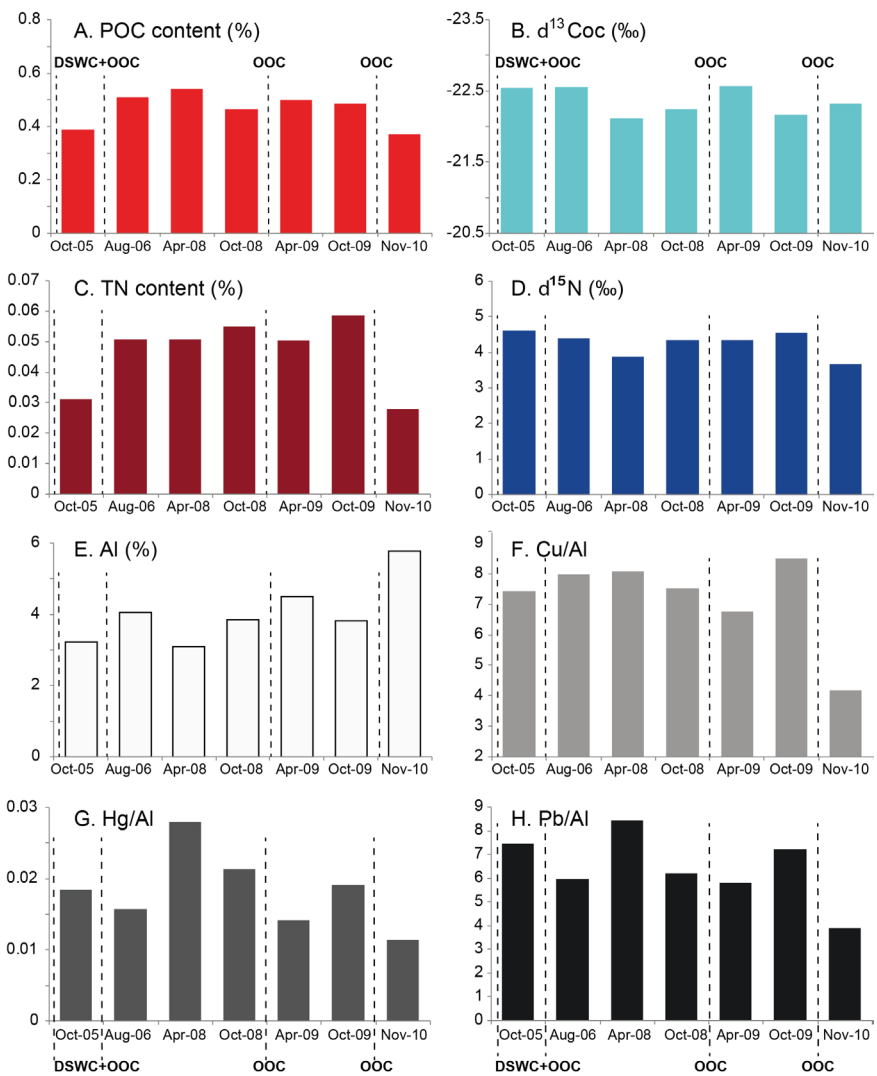

Fig. 3: Temporal pattern of sediment composition at site CCC1900 (see Figure 1 for the station location). Parameters for sediment organic composition: (A) POC (%), (B) $\delta^{13}C_{POC}$ (‰), (C) TN (%), (D) $\delta^{15}N$ (‰), and for sediment metal composition: (E) Al (%), (F) Cu/Al, (G) Hg/Al, (H) Pb/Al. The occurrence of winter DSWC and OOC events (dotted lines) are indicated.

Table 2. Temporal variability (TEMP): Core locations, pelitic fraction (%), POC (%), $\delta^{13}C_{POC}$ (‰), TN (%), $\delta^{15}N$ (‰), Al (%), Cu (µg/g), Hg (ng/g), and Pb (µg/g) content of surface sediment from October 2005 to November 2010 at coring station CCC1900. N = number of analytical replicates. Note that for comparison with other studies the values of the Cu/Al, Hg/Al and Pb/Al ratios must be multiplied by a factor of 10^{-4} to account for the units.

Coring site	Cruise	Lat	Long	Pelitic Fraction (%)	POC (%)	$\delta^{13}C_{POC}$ (‰)	TN (%)	$\delta^{15}N$ (‰)	Al (%)	Cu (µg/g)	Cu/Al	Hg (ng/g)	Hg/Al	Pb (µg/g)	Pb/Al
					n≥2	n≥5	n≥3	n≥4	n≥2	n≥2	n≥2	n≥2	n≥2	n≥2	n≥2
CCC1900	Oct-05	42.2147	4.2572	63.28	0.39	-22.54	0.031	4.60	3.22	24.0	7.45	59.5	0.018	24.1	7.49
	Aug-06	42.2155	4.2652	81.98	0.51	-22.56	0.051	4.40	4.06	32.5	8.00	64.0	0.016	24.4	6.00
	Apr-08	42.2148	4.2571	92.56	0.54	-22.11	0.051	3.89	3.10	25.0	8.08	86.8	0.028	26.2	8.46
	Sep-08	42.2145	4.2572	84.62	0.47	-22.25	0.055	4.34	3.85	29.0	7.54	82.3	0.021	24.0	6.24
	Apr-09	42.2148	4.2569	90.54	0.50	-22.57	0.050	4.35	4.50	30.5	6.77	63.8	0.014	26.2	5.83
	Oct-09	42.2145	4.2568	89.46	0.48	-22.17	0.059	4.57	3.83	32.6	8.52	73.4	0.019	27.7	7.23
	Nov-10	42.2171	4.2568	87.86	0.37	-22.32	0.028	3.67	5.78	24.1	4.18	66.1	0.011	22.6	3.90
	Mean ± sdt dev			84.33±9.9	0.47±0.06	-22.36±0.20	0.046±0.012	4.26±0.35	4.05±0.90	28.2±3.8	7.22±1.45	70.8±10.3	0.018±0.005	25.0±1.7	6.45±1.5
	Min			63.28	0.37	-22.57	0.028	3.67	3.10	24.0	4.18	59.5	0.011	22.6	3.90
	Max			92.56	0.54	-22.11	0.059	4.60	5.78	32.6	8.52	86.8	0.028	27.7	8.46
	CV (%)			11.7	13.5	-0.9	25.8	8.2	22.3	13.6	20.1	14.6	30.1	6.9	22.7

(November 2010) and 8.52 (October 2009), Pb/Al ranged between 3.90 (November 2010) and 8.46 (April 2008), and Hg/Al varied between 0.011 (November 2010) and 0.028 (April 2008). Comparison of coefficients of variation (CVs) (Table 2) allows to compare the variability between different parameters with different units. Highest CVs are observed for TN content, as well as for Al and the elements normalized by the aluminium. The highest CV for TN compared to POC may be explained by the low amount of injected TN (about ten times less than POC) within samples and therefore, to its proximity with the detection limit.

Large-scale variability of surface sediment across the slope (TRANSECT)

Large-scale spatial variability in Cap de Creus Canyon (3 cores from 1000 to 1900 m depth) and along the Southern Open Slope (13 cores from 150 to 2400 m depth) is presented in Figure 4 and Table 3.

The surface sediments along the Southern Open Slope to a depth of 1500 m are siltier and less sandy (clays ~ 21%, silts ~ 68%, sands ~ 11%) than those from deeper on the slope, particularly sediments in the basin (clays ~ 19%, silts ~ 61%, sands ~ 20%).

Here too, the spatial variability of the different elements indicates no common trend. POC contents varied between 0.47% (SOS1950) and 0.68% (SOS250) and $\delta^{13}C_{POC}$ ranged between -22.95‰ (SOS250) and -21.83‰ (SOS1950). TN contents varied between 0.051% (SOS1000) and 0.085% (SOS250) and $\delta^{15}N$ ranged between 3.89‰ (SOS1000) and 5.42‰ (SOS500). Lowest organic matter (TN and POC contents) concentrations were found at depths between 1900 and 2050 m.

Aluminium varied between 3.17% (SOS150) and 6.54% (SOS1300), with higher values (> 6%) being found at depths of between 500 and 1500m. Cu/Al ratios ranged between 3.19 (SOS500) and 8.56 (SC2400) and increased steadily downslope. Hg/Al ratios ranged between 0.008 (SOS1300) and 0.023 (SW2050), and no specific spatial trend was observed for this contaminant. Pb/Al ratios ranged between 4.39 (SOS1300) and 11.13 (SOS150): the lower values (<5) were found between 1000 and 1300 m depth and the highest value at SOS150 is twice as high as any other value. Minimum values of the trace metal to aluminium ratio were found at 1300 m depth, probably due to the maximal concentration of Al found there.

Highest CVs (Table 3) are observed for Al and the elements normalized by the aluminium. The organic matter composition presented less variability than did the metallic composition.

Small-scale variability of surface sediment at site CCC1900 (STATS)

Small-scale spatial variability of surface sediment composition at site CCC1900 is presented in Figure 5 and detailed in Table 4.

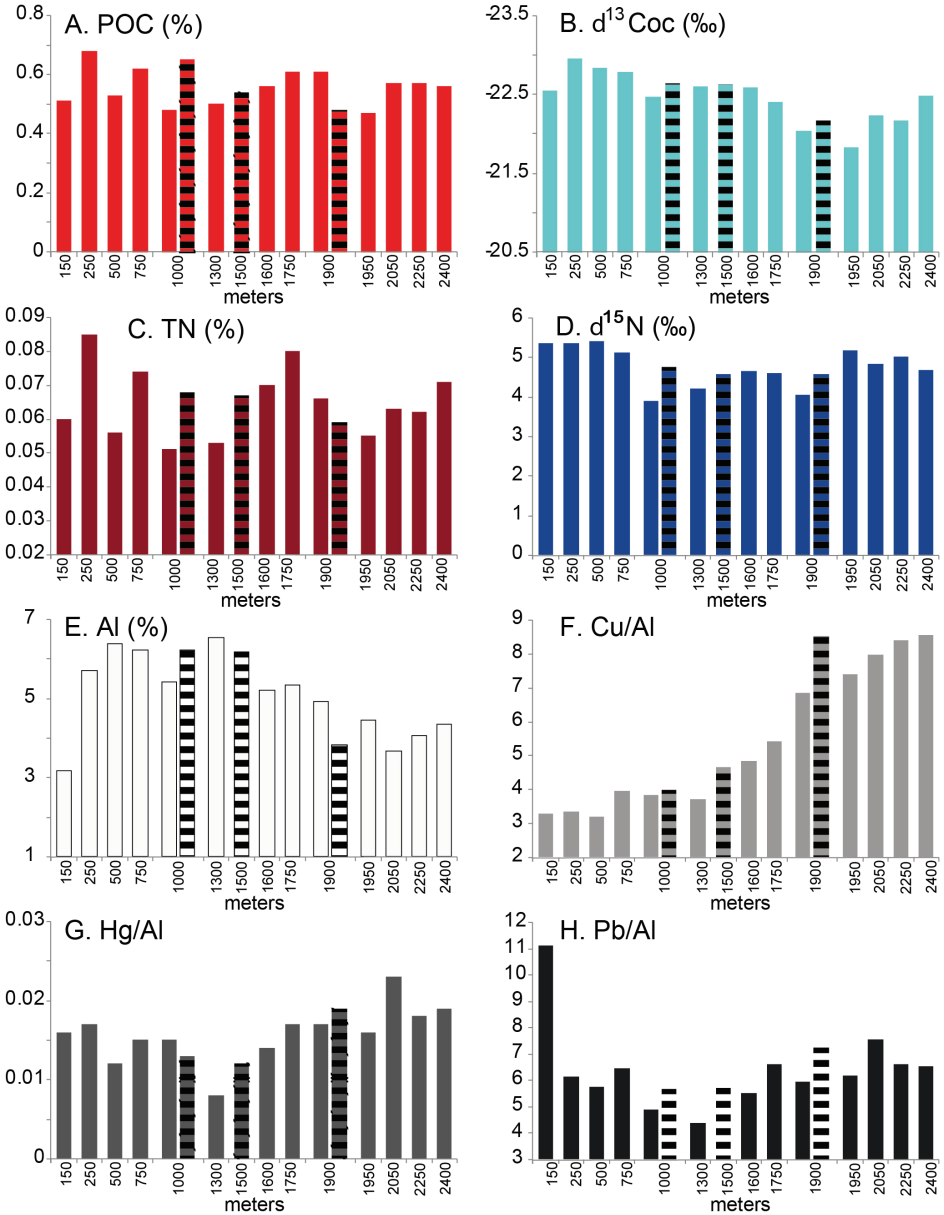

Fig. 4: Distribution of sediment organic composition (A) POC (%), (B) $\delta^{13}C_{POC}$ (‰), (C) TN (%), (D) $\delta^{15}N$ (‰), and sediment metal composition (E) Al (mg/g), (F) Cu/Al, (G) Hg/Al, (H) Pb/Al along two bathymetric transects: from 150 to 2400 m depth on the Southern Open Slope (plain bars), and from 1000 to 1900 m depth in Cap de Creus Canyon (dashed bars).

As was seen for the other stations, surface sediment at site CCC1900 is composed of silty loam (clays ~ 21%, silts ~ 54%, sands ~ 25%).

POC contents varied between 0.42 ± 0.02% (Deployment 3) and 0.59 ± 0.12% (Deployment 5), and $\delta^{13}C_{POC}$ ranged between -22.99 ± 0.03‰ (Deployment 5) and -22.13 ± 0.02‰ (Deployment 3) (Figure 5). Both POC contents ($p < 0.05$) and $\delta^{13}C_{POC}$ values ($p < 0.01$) differed significantly among deployments at the same site (PERMANOVA, Table 5). TN contents varied between 0.062 ± 0.003% (Deployment 1) and 0.045 ± 0.004% (Deployment 9), and $\delta^{15}N$ ranged between 4.27 ± 0.21‰ (Deployment 1) and 4.78 ± 0.21‰ (Deployment 8). PERMANOVA (Table 5) showed no significant difference between sites or deployments at this same site.

Aluminium, measured at each deployment, varied between 3.9% ± 0.3 (Deployment 9) and 5.0% ± 0.2% (Deployment 6); PERMANOVA results showed no significant difference between Al concentration between different sites and different deployments within the same site. Hg/Al ranged between 0.012 ± 0.001 (Deployment 4) and 0.018 ± 0.001 (Deployment 9), and PERMANOVA results revealed the presence of a statistical difference in the Hg/Al ratio ($p < 0.01$) between deployments at the same site. Pb/Al ranged between 5.2 ± 0.5 (Deployment 1) and 7.2 ± 0.9 (Deployment 9). Pb/Al ratios differed significantly ($p < 0.05$) between deployments at each site. Cu/Al ranged between 6.4 ± 0.3 (Deployment 1) and 7.6 ± 0.2 (Deployment 9). PERMANOVA results indicated a similarity between Cu/Al ratios between deployments within the same site. For all measured parameters, PERMANOVA showed no significant differences between sites.

Comparison of coefficients of variation (CVs) (Table 4) allows to compare the variability between differ-

Table 3. Large-scale spatial variability (TRANSECT): Core locations, pelitic fraction (%), POC (%), $\delta^{13}C_{POC}$ (‰), TN (%), $\delta^{15}N$ (‰), Al (%), Cu (µg/g), Cu/Al, Hg (ng/g), Hg/Al and Pb (µg/g), Pb/Al measurements of surface sediment from the bathymetric Southern Open Slope transect (150 to 2400 m depth) in October 2009. N = number of analytical replicates. Note that for comparison with other studies the values of the Cu/Al, Hg/Al and Pb/Al ratios must be multiplied by a factor of 10^{-4} to account for the units.

Coring site	Lat	Long	Pelitic Fraction (%)	POC (%)	$\delta^{13}C_{POC}$ (‰)	TN (%)	$\delta^{15}N$ (‰)	Al (%)	Cu (µg/g)	Cu/Al	Hg (ng/g)	Hg/Al	Pb (µg/g)	Pb/Al
				n≥2	n≥5	n≥3	n≥4	n≥2	n≥2	n≥2	n≥2	n≥2	n≥2	n≥2
SOS150	42.1538	3.4596	79.90	0.51	-22.55	0.060	5.36	3.17	10.4	3.29	50.1	0.016	35.3	11.13
SOS250	42.1487	3.5209	84.70	0.68	-22.95	0.085	5.35	5.70	19.1	3.34	98.3	0.017	35.0	6.14
SOS500	42.1355	3.6075	90.30	0.53	-22.83	0.056	5.42	6.38	20.4	3.19	76.3	0.012	36.6	5.73
SOS750	42.1280	3.7148	95.90	0.62	-22.78	0.074	5.11	6.23	24.6	3.94	96.5	0.015	40.3	6.47
SOS1000	42.1278	3.7750	95.50	0.48	-22.47	0.051	3.89	5.41	20.8	3.84	80.2	0.015	26.3	4.87
CCC1000	42.3074	3.6106	83.50	0.65	-22.64	0.068	4.76	6.23	24.9	4.00	80.6	0.013	35.4	5.67
SOS1300	42.1269	3.8030	92.50	0.50	-22.60	0.053	4.22	6.54	24.3	3.71	51.1	0.008	28.8	4.39
CCC1500	42.2165	3.8200	93.10	0.54	-22.63	0.067	4.57	6.17	28.8	4.67	75.1	0.012	35.3	5.72
SOS1600	42.1248	3.8565	93.50	0.56	-22.59	0.070	4.65	5.22	25.3	4.84	73.7	0.014	28.7	5.50
SOS1750	42.1229	3.9497	87.10	0.61	-22.41	0.080	4.61	5.34	28.9	5.42	88.8	0.017	35.2	6.60
SOS1900	42.1174	4.0457	85.80	0.61	-22.04	0.066	4.05	4.92	33.6	6.84	84.8	0.017	27.4	5.94
CCC1900	42.2145	4.2568	89.46	0.48	-22.17	0.059	4.57	3.83	32.6	8.52	73.4	0.019	27.7	7.23
SOS1950	42.1187	4.1834	76.60	0.47	-21.83	0.055	5.18	4.45	33.0	7.41	72.4	0.016	27.7	6.16
SW2050	42.1198	4.3201	80.30	0.57	-22.23	0.063	4.83	3.68	29.3	7.97	84.6	0.023	27.4	7.54
SOS2250	42.0749	4.4999	70.70	0.57	-22.17	0.062	5.01	4.05	34.0	8.39	73.3	0.018	27.7	6.61
SC2400	42.0331	4.6998	68.80	0.56	-22.48	0.071	4.67	4.35	37.3	8.56	83.2	0.019	26.8	6.52
		Mean ± sdt dev	85.50±8.4	0.56±0.06	-22.46±0.3	0.065±0.010	4.77±0.46	5.10±1.08	26.7±6.9	5.50±2.08	77.7±13.2	0.016±0.003	31.4±4.6	6.39±1.5
		Min	68.80	0.47	-22.95	0.051	3.89	3.17	10.4	3.19	50.1	0.008	26.3	4.39
		Max	95.90	0.68	-21.83	0.085	5.42	6.54	37.3	8.56	98.3	0.023	40.3	11.13
		CV (%)	9.8	11.3	-1.4	14.7	9.7	21.1	25.9	37.9	17.0	22.3	14.6	23.4

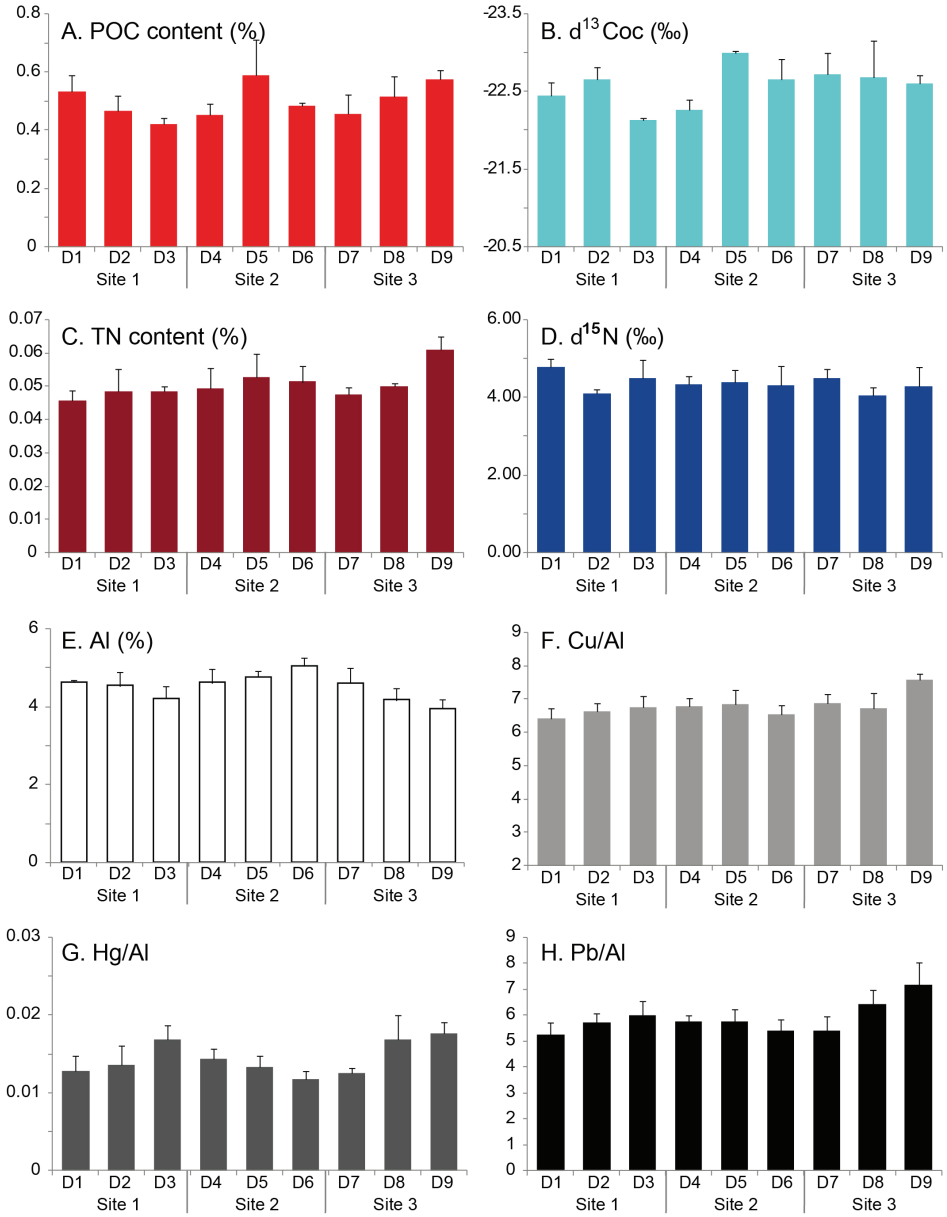

Fig. 5: Small-scale spatial pattern of sediment composition illustrated for organic composition by (A) POC (%), (B) $\delta^{13}C_{POC}$ (‰), (C) TN (%), (D) $\delta^{15}N$ (‰), and for metal composition by (E) Al (%), (F) Cu/Al, (G) Hg/Al, (H) Pb/Al at site CCC1900. Values are averaged over pseudo-replicates (3 cores within a multicorer deployment), and error bars denote the standard deviations. See Figure 2 for deployment and site locations.

ent parameters with different units. Highest CVs are observed for POC (15%) and Hg/Al (13%), medium CVs for TN (11%), Al (10%), $\delta^{15}N$ (8.1%), Pb/Al (8%) and Cu/Al (8%) and lowest for the $\delta^{13}C_{POC}$ (1%).

The experimental semi-variograms (Fig. 6) fluctuated randomly from the small scale (tens of centimeters) to the largest scales (hundreds of meters) for all parameters. The variability between i) three adjacent cores within a deployment, ii) between three deployments within a site, and iii) between three sites within the station was comparable and did not show any spatial pattern of the variability.

Discussion

The questions we will discuss herein are: (i) How do the observed organic matter and metal concentrations in superficial sediments compare with the values on the nearby shelf region?, (ii) How do the temporal changes of the geochemical composition of surface sediment in the lower reaches of Cap de Creus Canyon compare to the small-scale spatial variability?, and iii) Are there any observable significant changes on the larger scale (i.e. cross-slope transect) linked to the recurrence of disturbances?

Table 4. Small-scale spatial variability (STATS): Core locations, pelitic fraction (%), POC (%), $\delta^{13}C_{POC}$ (‰), TN (%), $\delta^{15}N$ (‰), Al (%), Cu (µg/g), Hg (ng/g), and Pb (µg/g) concentrations and Cu/Al, Hg/ Al, and Pb/Al ratios of surface sediment in April 2009. N = number of analytical replicates. Note that for comparison with other studies the values of the Cu/Al, Hg/Al and Pb/Al ratios must be multiplied by a factor of 10^{-4} to account for the units.

Coring site CCC1900	Lat	Long	Pelitic Fraction (%)	POC (%)	$\delta^{13}C_{POC}$ (‰)	TN (%)	$\delta^{15}N$ (‰)	Al (%)	Cu (µg/g)	Cu/Al	Hg (ng/g)	Hg/Al	Pb (µg/g)	Pb/Al
				n≥2	n>5	n>2	n>3	n≥2	n≥2	n≥2	n≥2	n≥2	n≥2	n≥2
D1_STAT1	42.2148	4.2569	82.30	0.59	-22.52	0.049	4.99	4.69	31.1	6.62	52.7	0.011	24.2	5.15
D1_STAT2	42.2148	4.2569	85.40	0.54	-22.25	0.046	4.57	4.62	30.2	6.55	68.6	0.015	26.5	5.75
D1_STAT3	42.2148	4.2569	75.70	0.48	-22.56	0.043	4.77	4.58	27.9	6.09	56.8	0.012	22.0	4.81
D2_STAT1	42.2152	4.2577	76.30	0.44	-22.79	0.042	4.19	4.13	26.1	6.32	67.0	0.016	25.2	6.09
D2_STAT2	42.2152	4.2577	82.40	0.52	-22.68	0.055	4.13	4.71	31.9	6.77	61.7	0.013	26.6	5.65
D2_STAT3	42.2152	4.2577	72.60	0.44	-22.48	0.048	3.99	4.76	32.1	6.75	53.3	0.011	25.7	5.40
D3_STAT1	42.2145	4.2577	74.30	0.40	-22.11	0.047	4.27	4.49	28.6	6.36	66.8	0.015	24.2	4.40
D3_STAT2	42.2145	4.2577	62.50	0.43	-22.15	0.056	4.18	3.85	26.7	6.94	64.9	0.017	23.7	6.15
D3_STAT3	42.2145	4.2577	69.30	0.44	-22.13	0.047	5.03	4.25	29.5	6.94	78.9	0.019	27.4	6.44
D4_STAT1	42.2179	4.2517	79.50	0.49	-22.15	0.056	4.10	5.02	35.3	7.04	67.1	0.013	29.1	5.81
D4_STAT2	42.2179	4.2517	81.40	0.41	-22.26	0.047	4.45	4.50	29.7	6.61	61.8	0.014	24.9	5.54
D4_STAT3	42.2179	4.2517	47.20	0.46	-22.39	0.045	4.47	4.31	28.8	6.68	67.9	0.016	25.6	5.95
D5_STAT1	42.2177	4.2523	82.10	0.53	-22.99	0.047	4.44	4.70	30.4	6.47	65.1	0.014	25.9	5.51
D5_STAT2	42.2177	4.2523	74.60	0.73	-22.97	0.061	4.05	4.62	33.8	7.32	66.6	0.014	29.0	6.28
D5_STAT3	42.2177	4.2523	82.50	0.51	-23.02	0.050	4.66	4.95	33.5	6.77	57.9	0.012	26.9	5.45
D6_STAT1	42.2178	4.2522	85.10	0.50	-22.63	0.046	4.88	4.82	32.8	6.81	62.2	0.013	27.6	5.72
D6_STAT2	42.2178	4.2522	80.40	0.47	-22.41	0.056	3.94	5.26	34.3	6.53	61.0	0.012	25.8	4.90
D6_STAT3	42.2178	4.2522	85.20	0.48	-22.92	0.052	4.08	5.03	31.5	6.26	53.9	0.011	28.1	5.58
D7_STAT1	42.2166	4.2537	79.60	0.41	-22.93	0.047	4.76	5.06	33.5	6.62	58.8	0.012	25.0	4.95
D7_STAT2	42.2166	4.2537	74.10	0.53	-22.82	0.050	4.32	4.37	31.3	7.15	55.2	0.013	26.3	6.02
D7_STAT3	42.2166	4.2537	74.20	0.42	-22.39	0.046	4.36	4.35	29.9	6.86	57.2	0.013	22.8	5.25
D8_STAT1	42.2168	4.2538	70.00	0.46	-22.22	0.049	3.81	4.18	28.2	6.74	84.5	0.020	27.2	6.50
D8_STAT2	42.2168	4.2538	57.20	0.59	-23.16	0.050	4.22	3.84	27.5	7.17	62.3	0.016	26.6	6.92
D8_STAT3	42.2168	4.2538	78.90	0.49	-22.66	0.051	4.11	4.47	28.1	6.29	62.5	0.014	26.4	5.90
D9_STAT1	42.2164	4.2539	67.60	0.60	-22.69	0.056	4.30	3.72	27.6	7.41	71.4	0.019	24.3	6.54
D9_STAT2	42.2164	4.2539	65.70	0.57	-22.63	0.064	3.74	3.88	29.1	7.48	65.3	0.017	26.5	6.83
D9_STAT3	42.2164	4.2539	70.50	0.54	-22.50	0.062	4.77	4.22	32.9	7.80	71.8	0.017	34.4	8.16
	Mean ± sdt dev		74.69±9.0	0.50±0.07	-22.57±0.31	0.051±0.006	4.35±0.35	4.50±0.41	30.5±2.5	6.79±0.41	63.8±7.5	0.014±0.003	26.2±2.4	5.84±0.77
		Min	47.20	0.40	-23.16	0.042	3.74	3.72	26.1	6.09	52.7	0.011	22.0	4.40
		Max	85.40	0.73	-22.11	0.064	5.03	5.26	35.3	7.80	84.5	0.020	34.4	8.16
		CV (%)	12.1	14.9	-1.4	11.4	8.1	9.0	8.2	6.0	11.7	17.8	9.0	13.2

Table 5. Non-parametric multivariate analyses of variance (PERMANOVA) of all the variables (using square root transformation and Hg, Cu, Pb variables), and of each variable separately (without transformation, and using Hg/Al, Cu/Al, Pb/Al) among sites and among deployments within each site. α-levels of 0.01, 4999 Monte-Carlo permutations. Source = source of variation, Df = Degree of freedom, SS = Sum of Square, MS = Mean Square, p(MC) = significance (ns, non-significant; * $p < 0.05$; ** $p < 0.01$; *** $p < 0.001$).

Variable	Source	Df	SS	MS	F	p(MC)
All (8)	Site	2	40.6630	20.3315	3.2506	ns
	Deployment (Site)	6	37.5282	6.2547	2.4451	ns
	Residual	18	46.0445	2.5580		
	Total	26	124.2357			
POC	Site	2	80.7227	40.3663	0.3710	ns
	Deployment (Site)	6	652.7631	108.7938	3.5671	*
	Residual	18	548.9935	30.4996		
	Total	26	1282.4893			
$\delta^{13}C_{POC}$	Site	2	1.7751	0.8875	0.8862	ns
	Deployment (Site)	6	6.0093	1.0016	4.1436	**
	Residual	18	4.3508	0.2417		
	Total	26	12.1351			
TN	Site	2	117.6229	58.8114	1.2323	ns
	Deployment (Site)	6	286.3516	47.7253	2.4415	ns
	Residual	18	351.8618	19.5479		
	Total	26	755.8364			
$\delta^{15}N$	Site	2	21.2285	10.6143	0.5008	ns
	Deployment (Site)	6	127.1667	21.1945	1.4136	ns
	Residual	18	269.8763	14.9931		
	Total	26	418.2716			
Al	Site	2	183.5678	91.7839	3.4421	ns
	Deployment (Site)	6	159.9924	26.6654	2.4755	ns
	Residual	18	193.8899	10.7717		
	Total	26	537.4501			
Cu/Al	Site	2	52.9834	26.4917	2.0713	ns
	Deployment (Site)	6	76.7387	12.7898	2.3720	ns
	Residual	18	97.0539	5.3919		
	Total	26	226.7760			
Hg/Al	Site	2	296.6699	148.3350	0.9291	ns
	Deployment (Site)	6	957.8873	159.6479	4.1811	**
	Residual	18	687.3016	38.1834		
	Total	26	1941.8589			
Pb/Al	Site	2	173.9793	86.9897	1.3486	ns
	Deployment (Site)	6	387.0183	64.5031	3.5909	*
	Residual	18	323.3289	17.9627		
	Total	26	884.3266			

Gradients of organic matter and metal concentrations in sediments between the coastal zone and the basin

Most of the organic matter found in superficial shelf sediment close to the river mouths in the Gulf of Lions is of terrigenous origin, with POC = 1.6 ± 0.28 %, $\delta^{13}C_{POC}$ = -26.6 ± 0.4‰. POC and $\delta^{13}C_{POC}$ show a gradient with distance from river sources and the presence of older and more degraded organic matter (POC = 1.0 ± 0.2 %, $\delta^{13}C_{POC}$ = -24.6 ± 0.9‰) (Cathalot *et al.*, 2013). Such values are higher than the values observed on the slope itself and in the basin (POC = 0.51 ± 0.08% , $\delta^{13}C_{POC}$ = -22.5 ± 0.3‰). DSWC events are concomitant with spring planktonic blooms on the continental shelf. Based on grain size, organic carbon (OC) and total nitrogen (TN) contents and their isotopic ratios ($\delta^{13}C_{POC}$ and $\delta^{15}N$), Sanchez-Vidal *et al.* (2009) and Pasqual *et al.* (2010) showed that large amounts of particulate matter are exported from the shelf during the DSWC pulses. Downslope fluxes of particulate matter are mostly composed of degraded organic matter with low $\delta^{13}C_{POC}$ (-22.55‰) and high $\delta^{15}N$ (6.6‰) values, originating in the sediment but resuspended by the strong bottom flow over the shelf. However, an input of fresh organic matter of planktonic origin, with high $\delta^{13}C_{POC}$ (22.19‰) and extremely low $\delta^{15}N$ (0.0‰) values, may also be present. Pusceddu *et al.* (2010) analysed the quantity and biochemical composition of the organic matter of surface sediments collected at different depths in Cap de Creus Canyon before (May 2004) and after (April 2005) the intense DSWC and OOC events of winter 2005. They reported that these events resulted in a significant depletion of the organic content of the canyon bottom sediments between 1000 and 1900 m depth, and in a significant increase in POC concentrations in the sediments further down the canyon at 2200 m depth. All these results suggest a significant difference in the quali-

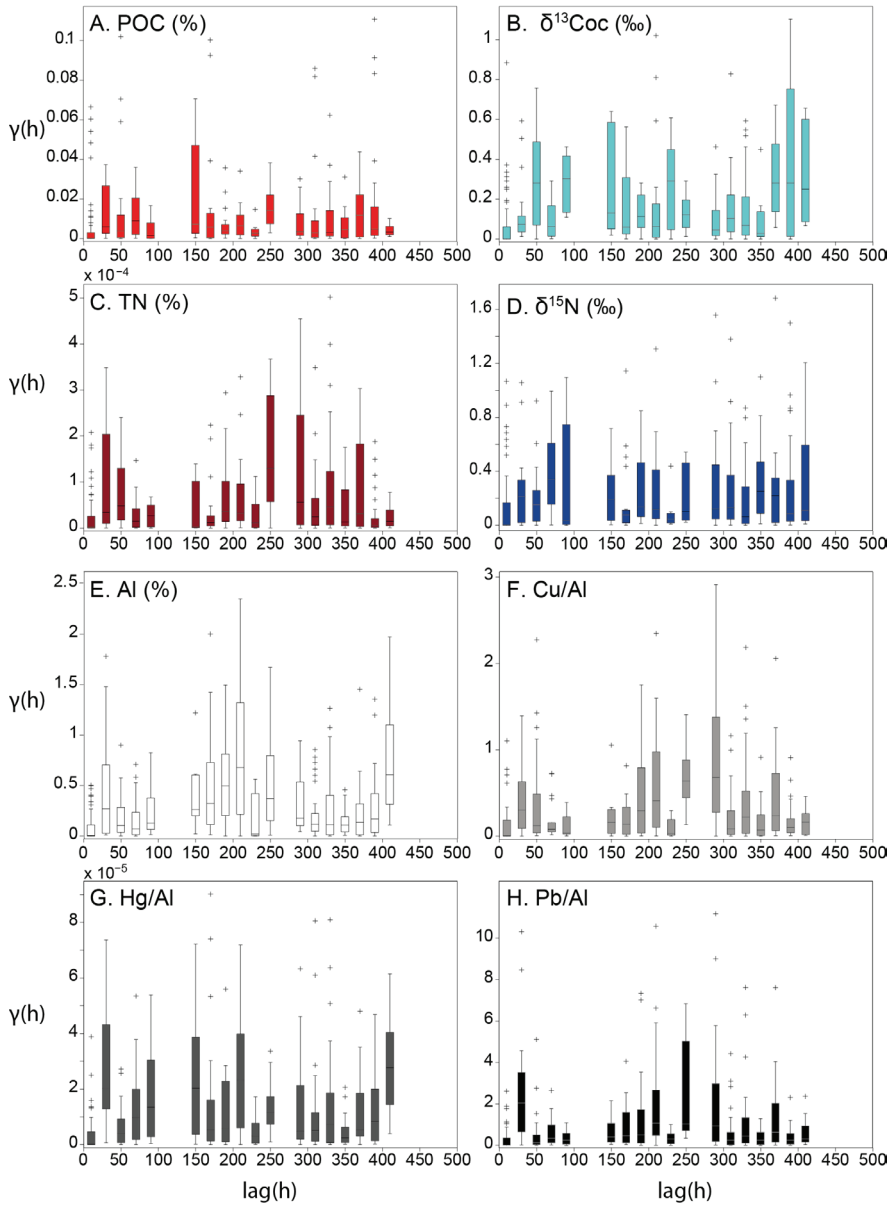

Fig. 6: Semi-variograms of (A) POC (%), (B) $\delta^{13}C_{POC}$ (‰), (C) TN (%), (D) $\delta^{15}N$ (‰), and sediment metal composition reported are (E) Al (%), (F) Cu/Al, (G) Hg/Al, (H) Pb/Al at site CCC1900 (bin = 20m).

ty of the organic matter sampled between the shelf adjacent to the studied slope and the basin sites. The intense DSWC and OOC events represent major processes that supply the seabed with organic matter that bears a distinct signature from that of deep sediments.

On the shelf of the Gulf of Lions, Cu and Pb concentration in the superficial sediment follow the depositional feature of the finest sediment fractions and their affinity with organic matter (Roussiez *et al.* 2006; Cossa *et al.* 2014). The highest concentrations are thus found in river prodeltas, which are very local, and on the shelf mudflats. The average concentration of Cu on the shelf, excluding the river prodelta, was assessed at 20.2 ± 6.5 µg/g (Roussiez *et al.* 2006), and 19.9 ± 3.9 µg/g (Cossa *et al.*, 2014). These values are lower than those found on the slope and in the basin (TRANSECT: 26.7 ± 6.9 µg /g ; TEMP: 28.2 ± 3.8 µg/g ; STATS: 30.5 ± 2.5 µg/g. Conversely, the average concentration of Pb on the shelf, excluding the river prodelta, was evaluated at 37.1 ± 7.5 µg/g (Roussiez *et al.* 2006), and 38.4 ± 4.9 µg/g (Cossa *et al.*, 2014). These values are higher than those observed for the surficial sediments of the slope and basin (TRANSECT: 31.4 ± 5.6 µg/g; TEMP: 25 ± 1.7 µg/g; STATS: 26.2 ± 2.4 µg/g). Likewise, Hg concentrations in superficial coastal sediments are generally higher than deep basin sediments (Kotnik *et al.*, 2014). In the Gulf of Lions, Hg concentration for the superficial sediment on the shelf was estimated at 172 ± 130 ng/g (Arnoux *et al.*, 1975), which is significantly higher than the concentrations observed on the slope and in the basin (TEMP: 70.8 ± 10.3 ng/g, TRANSECT :77.7 ± 13.2 ng/g, and STATS: 63.8 ± 7.5 ng/g). We can thus see differences in the average concentrations of the metallic elements presented here from the adjacent continental shelf and the study area. The downslope export of sedimentary material from the plateau during intense DSWC events is therefore likely to modify the geochemical signature of the deep sediments.

Comparison of the studied variabilities

Comparison of all studied variability groups (STATS, TEMP and TRANSECT) for each variable is summarized in Figure 7. As can be visually inferred from the histograms (Figs 3, 4, and 5), there are differences in the range of variability between the studied variables, mostly for large-scale variability (TRANSECT). The highest variability along this cross-slope transect was found for Al and Cu/Al, whereas for the other variables similar variability is observable between the three groups. It remains difficult to determine which distribution is different or similar to the other without performing a supplementary statistical test.

The results of the Kruskal-Wallis (degree of freedom = 2, N = 51) analysis (Table 6) indicated that there is a significant difference in the medians of the three groups for the variable Cu/Al, POC, TN, $\delta^{15}N$, and Al. Because the test is significant, post-hoc pairwise comparisons within the three groups should be completed for these variables (Table 7).

Surprisingly, temporal (TEMP) vs. small-scale (STATS) variability is never significant (ns, Table 7). Statistical tests show that, for all the elements, small-scale spatial variability does not differ from temporal variability. The difference in the measurements between two adjacent cores from the same multicorer deployment is similar to the differences between deployments and sites at station CCC1900. The range of variation between all 27 cores is larger than the range of variation due to temporal variability, indicating that small-scale heterogeneity of the sediment masks the observed temporal variability. This result clearly illustrates the need to take into account the intrinsic variability of the studied environment, in addition to being rigorous regarding the accuracy of the measurements.

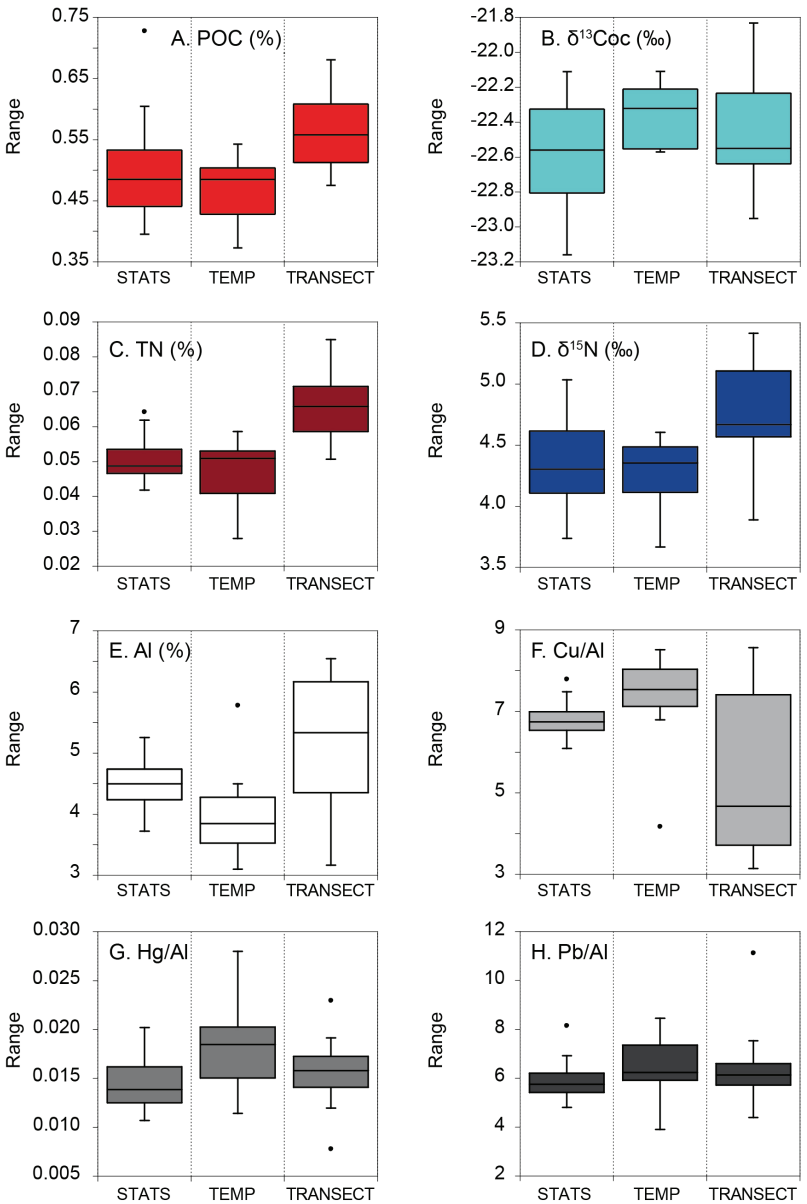

Fig. 7: Box plots (around the median) of the three sources of variability: small-scale variability at CCC1900 (STATS), temporal variability at CCC1900 (TEMP), and large-scale bathymetric variability (TRANSECT) for sediment organic composition (A) POC, (B) $\delta^{13}C_{POC}$, (C) TN, (D) $\delta^{15}N$, and sediment metal distribution (E) Al, (F) Cu/Al, (G) Hg/Al, (H) Pb/Al. Note the outliers (black dots).

Table 6. Results of the Kruskal-Wallis (Chi² approximation method) test for each parameter. H is the Kruskal-Wallis statistic, p the p-values *** = $P < 0.001$; ** = $p < 0.01$, $p < 0.05$.

A = 0.05	POC	$\delta^{13}C_{POC}$	TN	$\delta^{15}N$	Al	Cu/Al	Hg/Al	Pb/Al
H	11.50	2.79	24.20	7.83	7.99	7.65	5.29	3.68
p-value	0.00318	0.2474	<0.0001	0.01997	0.01841	0.02185	0.07097	0.15869
Significance	**	ns	***	*	*	*	ns	ns

Table 7. Post-hoc pair-wise comparison to contrast source of variation STATS (n=27), TEMP (n=7), and TRANSECT (n= 16) for variables that presented significant differences after the KW test (POC, TN, $\delta^{15}N$, Al, Cu/Al).

Variable	Source	Observed Difference	Critical Difference	Significance
POC	STATS - TEMP	4.47	15.09	ns
	STATS - TRANSECT	13.73	11.02	*
	TEMP- TRANSECT	18.19	15.98	*
TN	STATS - TEMP	1.20	15.09	ns
	STATS - TRANSECT	21.95	11.02	*
	TEMP- TRANSECT	20.76	15.98	*
$\delta^{15}N$	STATS - TEMP	2.98	15.09	ns
	STATS - TRANSECT	11.56	11.02	*
	TEMP- TRANSECT	14.55	15.98	ns
Al	STATS - TEMP	9.73	15.09	ns
	STATS - TRANSECT	8.43	11.02	ns
	TEMP- TRANSECT	18.18	15.98	*
Cu/Al	STATS - TEMP	10.82	15.09	ns
	STATS - TRANSECT	7.35	11.02	ns
	TEMP- TRANSECT	18.17	15.98	*

Likewise, for most elements, the tests indicate that there is no significant difference between the small-scale spatial variability and variability on a larger scale (across the slope). The differences between the STATS and TRANSECT groups for Al and Cu/Al ratio variables were clearly related to downslope trends in Al and Cu concentrations. The notable increase in silt fraction and aluminium content in the upper part of the slope (between 100 and 1500 m) suggests that there may indeed be an effect due to recurring DSWC events. The differences for POC, TN and $\delta^{15}N$ are not the result of strong trends, as was seen for Al and Cu; rather, the concentrations of these elements across the slope are highly variable from station to station, with the mean value ultimately showing an increase due to the incorporation of anomalous measurements from certain stations.

Potential origins of small- and large-scale variations

The study of temporal and small-scale variability at site CCC1900 was performed on the upper 0.5 cm, which corresponds approximately to the past ten years of depositional flux, given a median accumulation rate of 0.1 cm/y (Miralles *et al.*, 2005). The surficial sediment sampling may be too thick (> 0.5 cm) for the perturbation induced by the studied DWF events. Furthermore, deep-sea sediments present small-scale microtopographies [e.g. Tubau *et al.* (2015)] and continuous reworking by bioturbation (Pusceddu *et al.*, 2013). This microhabitat heterogeneity greatly influences the diversity found in the sedimentary and geochemical composition replicates. Any sampling strategy has to be adapted to take this small-scale patchiness into account, so as to allow for the correct assessment of the surface sediment measurements. Sample pooling and master cores are generally the most cost-effective solutions (Kelly *et al.*, 1994).

The origin of the change in sediment characteristics across the open slope to 1500 m depth may be due to various factors. A recent study (Ribó *et al.*, 2018) has shown that the outer continental shelf and upper slope south of Cap de Creus Canyon is characterized both by morphological erosional features and by large sediment waves between ~200 and ~400 m-depth. Those authors associated these erosional features with bottom currents, which intensify during DSWC events and storm-induced downwelling. These downwelling and cascading events affecting the upper continental slope are events of almost

annual occurrence, while deep cascading events are much less frequent.

Moreover, the slope south of Cap de Creus Canyon is also prone to intense bottom trawling, mostly between 150 and 550 m. The sustained alteration of sediments induced by trawling further contributes to changes in the physical and geochemical properties of surface sediments. This may also lead to impoverishment of the chemical bond between Cu and organic matter through enhanced desorption processes during sediment resuspension (Dang *et al.*, 2020).

Hence, recurrent resuspension of sediment can result in the winnowing of the finest sediments fraction, and in its near-bottom transport towards deeper depocenters.

Conclusions

The Gulf of Lions is a unique site which enables, first of all, to determine if and how surface sediments can be studied to follow the potential impact of DWF events on the geochemical composition of surface sediments on slopes and in basins, and secondly, on an even broader scale, what information can be inferred from surface sediment analysis.

Our results underline that severe DWF events do not yield detectable changes in surface sediment geochemical composition on the lower slope and basin of the Gulf of Lions, because any changes are masked by the high small-scale variability of the surface sediment. Indeed, variability at decimetric, decametric and hectometric scales of surface sedimentological (grain size) and biogeochemical (metals, organic matter) characteristics is comparable, and does not appear to be significantly different from temporal (interannual) variability at the same site.

This small-scale patchiness, although recognized, is rarely taken into account in sedimentological studies. However, its omission can lead to interpretation bias in studies conducted on a single core, yet intended to reflect a given environment. Taking into account the intrinsic spatial heterogeneity of sediment -at the decimetric scale- is thus a requisite for suitable observations of temporal changes. Moreover, sufficient replications are required to fully take into consideration the scale and magnitude of this intrinsic variability, and to show that it is smaller than the variability which is being interpreted (temporal surface, sediment archive, larger spatial scales).

Acknowledgements

This research was funded by the HERMES (Hotspot ecosystem research on the margins of European seas, IP FP6-SUSTDEV) and HERMIONE (Hotspot Ecosystem Research and Man's Impact On European Seas, IP-FP7- FP7-ENVIRONMENT) projects. We acknowledge the technical support of Gérard Gentil, and Christine Sotin.

References

Anderson, M.J., 2001. Permutation tests for univariate or multivariate analysis of variance and regression. *Journal canadien des sciences halieutiques et aquatiques*, 58 (3), 626-639.

Anderson, M.J., Braak, C.T., 2003. Permutation tests for multi-factorial analysis of variance. *Journal of Statistical Computation and Simulation*, 73 (2), 85-113.

Anderson, M. J., Robinson, J., 2003. Generalized discriminant analysis based on distances. *Australian & New Zealand Journal of Statistics*, 45, 301-318.

Angelidis, M.O., Radakovitch, O., Veron, A., Aloupi, M., Heussner, S. *et al.,* 2011. Anthropogenic metal contamination and sapropel imprints in deep Mediterranean. *Marine Pollution Bulletin*, 62 (5), 1041-1052.

Arnoux, A., Gilles, G., Ramonda, G., 1975. Pollution par le mercure des sediments superficiels du golfe du Lion. *Comptes Rendus de l'Académie des Sciences*, Paris, 281, Série D, 743-746.

Barnett, P.R.O., Watson, J., Connelly, D., 1984. A multiple corer for taking virtually undisturbed samples from shelf, bathyal and abyssal sediments. *Oceanologica Acta*, 7 (4), 399-408.

Béthoux, J.P., Durrieu de Madron, X., Nyffeler, F., Taillez, D., 2002. Deep water in the western Mediterranean: peculiar 1999 and 2000 characteristics, shelf formation hypothesis, variability since 1970 and geochemical inferences. *Journal of Marine Systems*, 33-34, 117-131.

Canals, M., Puig, P., Durrieu de Madron, X., Heussner, S., Palanques, A. *et al.*, 2006 Flushing submarine canyons. *Nature*, 444, 354-357.

Cathalot, C., Rabouille, C., Tisnerat-Laborde, N., Toussaint, F., Kerhervé, P. *et al.,* 2013. The fate of river organic carbon in coastal areas: A study in the Rhône River delta using multiple isotopic ($\delta^{13}C$, $\Delta^{14}C$) and organic tracers. *Geochimica et Cosmochimica Acta*, 118, 33-55.

Cossa, D., Buscail, R., Puig, P., Chiffoleau, J.F., Radakovitch, O. *et al.,* 2014. Origin and accumulation of trace elements in sediments of the northwestern Mediterranean margin. *Chemical Geology*, 380, 61-73.

Dang, D.H., Layglon, N., Ferretto, N., Omanovic, D., Mullot, J.U., *et al.*, 2020. Kinetic processes of copper and lead remobilization during sediment resuspension of marine polluted sediments. *Science of the Total Environment*, 698, 134120.

Dumas, C., Aubert, D., Durrieu de Madron, X., Ludwig, W., Heussner, S. *et al.,* 2014. Storm-induced transfer of particulate trace metals to the deep-sea in the Gulf of lion (NW Mediterranean Sea). *Environmental Geochemistry and Health*, 36 (5), 995-1014.

Durrieu de Madron, X., Houpert, L., Puig, P., Sanchez-Vidal, A., Testor, P. *et al.,* 2013. Interaction of dense shelf water cascading and open-sea convection in the Northwestern Mediterranean during winter 2012. *Geophysical Research Letters*, 40, 1379-1385.

Durrieu de Madron, X., Ramondenc, S., Berline, L., Houpert, L., Bosse, A. *et al.,* 2017. Deep sediment resuspension and thick nepheloid layer generation by open-ocean convection. *Journal of Geophysical Research – Oceans,* 122, 2291-2318.

Durrieu de Madron, X., Wiberg, P., Puig, P., 2008. Sediment dynamics in the Gulf of Lions: The impact of extreme events. *Continental Shelf Research*, 28, 1867-1876.

Durrieu de Madron, X., Zervakis, V., Theocharis, A., Georgopoulos, D., 2005. Comments to "Cascades of dense water around the world ocean". *Progress in Oceanography*, 64 (1), 83-90.

Georgin, P., Mouet, M., 2000 Statistiques avec Excel. Eyrolles ed. *Presses Universitaires de Rennes*, Paris, France, 344p.

Heimbürger, L-A., Migon, C., Losno, R., Miquel, J-C., Thibodeau, B. *et al.,* 2014. Vertical export flux of metals in the Mediterranean Sea. *Deep Sea Research*, 87, 14-23.

Houpert, L., Durrieu de Madron, X., Testor, P., Bosse, A., D'Ortenzio, F. *et al.,* 2016. Observations of open-ocean deep convection in the Northwestern Mediterranean Sea seasonal and interannual variability of mixing and deep water masses for the 2007-2013 period. *Journal of Geophysical Research - Oceans*, 121, 8139- 8171.

Kelly, A.G., Wells, D.E., Fryer, R.J., 1994. Sampling strategy to detect a change in concentration of trace organic contaminants in marine sediment. *Science of The Total Environment*, 144 (1-3), 217-230.

Kotnik, J., Sprovieri, F., Ogrinc, N., Horvat, M., Pirrone, N., 2014. Mercury in the Mediterranean, part I: spatial and temporal trends. *Environmental Science and Pollution Research*, 21, 4063-4080.

Lochte, K., Anderson, R., Francois, R., Jahnke, R.A., Shimmield, G. *et al.,* 2003. Benthic Processes and the Burial of Carbon. In: Fasham M.J.R. (eds) *Ocean Biogeochemistry. Global Change - The IGBP Series* (closed). Springer, Berlin, Heidelberg. 195-216.

Lopes-Rocha, M., Langone, L., Miserocchi, S., Giordano, P., Guerra, R., 2017. Detecting long-term temporal trends in sediments-bound metals in the western Adriatic (Mediterranean Sea). *Marine Pollution Bulletin*, 124 (1), 270-285.

Loring, D.H., 1991. Normalization of heavy-metal data from estuarine and coastal sediments. *ICES Journal of Marine Science*, 48, 101-115.

Martín, J., Sanchez-Cabeza, J.A., Eriksson, M., Levy, I., Miquel, J.-C., 2009. Recent accumulation of trace metals in sediments at the DYFAMED site (Northwestern Mediterranean Sea). *Marine Pollution Bulletin*, 59 (4-7), 146-153.

Miralles, J., Radakovitch, O., Aloisi, J.-C., 2005. ^{210}Pb sedimentation rates from the Northwestern Mediterranean margin. *Marine Geology*, 216 (3), 155-167.

Miralles, J., Veron, A., Radakovitch, O., Deschamps, P., Tremblay, P. *et al.,* 2006. Atmospheric lead fallout over the last century recorded in Gulf of Lions sediments (Mediterranean Sea). *Marine Pollution Bulletin*, 52 (11), 1364-1371.

Nardelli, M., Sabbatini, A., Bonnot, E., Mea, M., Pusceddu, A. *et al.,* 2018. Benthic foraminiferal assemblages in the Cap de Creus canyon and adjacent open slope: Potential influence of dense shelf water cascading and open-ocean convection. *Deep Sea Research*, 136, 31-43.

Olsen, C.R., Cutshall, N.H., Larsen, I.L., 1982. Pollutant-particle associations and dynamics in coastal marine environments: a review. *Marine Chemistry*, 11 (6), 501-533.

Palanques, A., Puig, P., Durrieu de Madron, X., Sánchez-Vidal, A., Pasqual, C. *et al.,* 2012. Sediment transport to the deep canyons and open-slope of the western Gulf of Lions during the 2006 intense cascading and open-sea convection period. *Progress in Oceanography*, 106, 1-15.

Palanques, A., Puig, P., 2018. Particle fluxes induced by benthic storms during the 2012 dense shelf water cascading and open sea convection period in the northwestern Mediterranean basin. *Marine Geology*, 406, 119-131.

Panogos, P., Ballabio, C., Lugato, E., Jones, A., Borrelli, P. *et al.,* 2018. Potential sources of anthropogenic copper inputs to European agricultural soils. *Sustainability*, 10, 2380.

Pasqual, C., Sanchez-Vidal, A., Zúñiga, D., Calafat, A., Canals, M. *et al.,* 2010. Settling particle fluxes across the continental margin of the Gulf of Lion: the role of dense shelf water cascading. *Biogeosciences*, 7, 217-231.

Puig, P., Durrieu de Madron, X., Salat, J., Schroeder, K., Martín, J. *et al.,* 2013. Thick bottom nepheloid layers in the western Mediterranean generated by deep dense shelf water cascading. *Progress in Oceanography*, 111, 1-23.

Pusceddu, A., Mea, M., Gambi, C., Bianchelli, S., Canals, M. *et al.,* 2010. Ecosystems effects of dense water formation on deep Mediterranean Sea ecosystems : an overview. *Advances in Oceanography and Limnology*, 1 (1), 67-83.

Pusceddu, A., Mea, M., Canals, M., Heussner, S., Durrieu de Madron, X. *et al.,* 2013. Major consequences of an intense dense shelf water cascading event on deep-sea benthic trophic conditions and meiofaunal biodiversity. *Biogeosciences*, 10, 2659-2670.

Ribó, M., Durán, R, Puig, P., Van Rooij, D., Guillén, J. *et al.,* 2018. Large sediment waves over the Gulf of Roses upper continental slope (NW Mediterranean). *Marine Geology*, 399, 84-96.

Roussiez, V., Ludwig, W., Monaco, A., Probst, J.L., Bouloubassi, R. *et al.,* 2006. Sources and sinks of sediments-bound contaminants in the Gulf of Lions (NW Mediterranean Sea): a muti-tracer approach. *Continental Shelf Research*, 26, 1843-1857.

Roussiez, V., Heussner, S., Ludwig, W., Radakovitch, O., Durrieu de Madron, X. *et al.,* 2012. Impact of oceanic floods on particulate metal inputs to coastal and deep-sea environments: a case study in the NW Mediterranean Sea. *Continental Shelf Research*, 45, 15-26.

Salvadó, J.A., López, J.L., Grimalt, J.O., Durrieu de Madron, X., Heussner, S. *et al.,* 2012 Transformation of PBDE mixtures during sediment transport and resuspension in marine environments (Gulf of Lion, NW Mediterranean Sea). Environmental Pollution, 168, 87-95.

Salvadó, J.A., Grimalt, J.O., Lopez, J.F., Durrieu de Madron, X., Pasqual, C. *et al.,* 2013. Distribution of organochlorine compounds in surficial sediments from the Gulf of Lion, northwestern Mediterranean Sea. *Progress in Oceanography*, 118, 235-248.

Sanchez-Vidal, A., Pasqual, C., Kerhervé, P., Heussner, S., Calafat, A. *et al.,* 2009. Across margin export of organic matter by cascading events traced by stable isotopes, northwestern Mediterranean Sea. *Limnology & Oceanography*, 54 (5), 1488–1500.

Siegel, S., Castellan, N.J. Jr., 2002. The case of one sample, two measures or paired replicates; in Siegel S, Castellan NJ Jr (eds): *Nonparametric Statistics for the Behavioral Sciences*, ed 2. Singapore, McGraw-Hill, pp 73-101.

Somot, S., Houpert, L., Sevault, F., Testor, P., Bosse, A. *et*

al., 2016. Characterizing, modelling and understanding the climate variability of the deep water formation in the North-Western Mediterranean Sea. *Climate Dynamics*, 51 (3), 1179-1210.

Stabholz, M., Durrieu de Madron, X., Khripounoff, A., Canals, M., Taupier-Letage, I. *et al.,* 2013. Impact of open-sea convection on particulate fluxes and sediment dynamics in the deep basin of the Gulf of Lions. *Biogeosciences*, 10, 1097-1116.

Testor, P., Bosse, A., Houpert, L., Margirier, F., Mortier, L. *et al.,* 2018. Multi-scale observations of deep convection in the northwestern Mediterranean Sea during winter 2012-2013 from a multi-platform approach. *Journal of Geophysical Research - Oceans*, 123, 1745-1776.

Tubau, X., Canals, M., Lastras, G., Rayo, X., Rivera, J. *et al.,* 2015. Marine litter on the floor of deep submarine canyons of the Northwestern Mediterranean Sea: The role of hydrodynamic processes. *Progress in Oceanography*, 134, 379-403.

Valette-Silver, N.J., 1993. The use of sediment cores to reconstruct historical trends in contamination of estuarine and coastal sediments. *Estuaries*, 16 (3), 577-588.

Van der Weijden, C.H., 2002. Pitfalls of normalization of marine geochemical data using a common divisor. *Marine Geology*, 184 (3-4), 167-187.